Zweitveröffentlichung/ Secondary Publication

Thamires Canuto de Almeida e Silva, Gourav Dhar Bhowmick, Makarand Madhao Ghangrekar, Michaela Wilhelm, Kurosch Rezwan

SiOC-based polymer derived-ceramic porous anodes for microbial fuel cells

Recommended Citation (primary publication/Version of Record) incl. DOI:

Take down policy

Regular article

SiOC-based polymer derived-ceramic porous anodes for microbial fuel cells

Thamires Canuto de Almeida e Silva[a], Gourav Dhar Bhowmick[b], Makarand Madhao Ghangrekar[c], Michaela Wilhelm[a,*], Kurosch Rezwan[a,d]

[a] *University of Bremen, Advanced Ceramics, Am Biologischen Garten 2, IW3, 28359, Bremen, Germany*
[b] *Department of Agricultural and Food Engineering, Indian Institute of Technology, 721302, Kharagpur, India*
[c] *Department of Civil Engineering, Indian Institute of Technology, 721302, Kharagpur, India*
[d] *MAPEX Center for Materials and Processes, University of Bremen, 28359, Bremen, Germany*

HIGHLIGHTS

- Novel polymer-derived ceramic based anode materials applied in MFCs.
- PDC-based anodes with porous structures and hydrophilic surfaces were developed.
- Maximum power density of 211 mW m^{-2} with 85% COD removal.

ARTICLE INFO

ABSTRACT

The applicability of a new class of ceramic materials in Microbial Fuel Cells (MFCs) was investigated, targeting the development of cost-effective anode materials with long-term durability. In this work, silicon oxycarbide (SiOC)-based porous anodes were prepared by the polymer-derived ceramics (PDCs) route, using poly(methyl silsesquioxane) and poly(methyl phenyl silsesquioxane) as precursors while incorporating carbonaceous fillers (graphite and carbon black) and metal precursor (NiCl$_2$). Tape casting was used in the manufacturing followed by pyrolysis at 1000 °C under nitrogen atmosphere. The interior structure and surface morphology were characterized with scanning electron microscopy (SEM), nitrogen adsorption, vapor adsorption, and contact angle measurements. The developed anodes were tested in MFC with aqueous cathode configuration using a low-cost clayware cylinder as the anodic chamber. The performance of MFC using PDC-based anodes was compared with MFC having carbon felt as anode material, which showed a two-fold increase in power density (211 and 111 mW m^{-2}, respectively) and normalized energy recovery in former and also demonstrated chemical oxygen demand (COD) removal efficiency of about 85%. The improved performance of the PDC-based anodes is attributed to its porous structure, hydrophilic surface, and high specific surface area (39.89 m^2 g^{-1}). The biocompatibility was confirmed by biofilm growth on the surfaces, while a sufficient electrical conductivity (0.10–0.18 S cm^{-1}) makes it superior electrode material for application in MFCs.

1. Introduction

Two major problems that humanity is now facing are environmental pollution and the energy crisis. Microbial fuel cells (MFCs) arise as a single system, wherein electricity is produced from the biomass using bacteria as biocatalyst, while the wastewater is treated [1]. The electricity generation occurs through the oxidation of organic matter present in the wastewater, and the release of electrons which are transferred to the anode due to the growth of exoelectrogenic bacteria on the anode surface. The electrons flow through an external circuit reaching the cathode, thus producing an electric current. Subsequently, the electrons combine with oxygen molecules, which act as a terminal electron acceptor, and with protons that were diffused through a proton exchange membrane [2,3]. The interaction of bacteria with the anode surface, the resistance of electron flow, and substrate oxidation essentially depend on the properties of anode materials. Therefore, the anode is the defining element that can critically affect the overall performance of an MFC [4–6]. In general, an ideal anode material should have good electrical conductivity, biocompatibility, large surface area, chemical stability, sufficient mechanical strength, and low costs [7]. The most reported anode materials used in MFCs are the traditional carbon-based materials, such as carbon cloth and felt, carbon brush, carbon rod and

granular activated carbon [6]. However, their inherently hydrophobic character and limited active reaction sites restrict microbial adhesion and biofilm formation. Additionally, the surface fouling of the material due to microbial secretion during the operation of MFC may cause the loss of anode functionality and, as a result, compromise the power output [8–10]. From this perspective, there have been great efforts in the development of novel anode materials that could provide better surface characteristics for biofilm formation and to improve electron transfer. Other properties such as optimized porous structure to accommodate bacteria cells and maintain the access of nutrients through the pores, and long-term stability, are also highly desirable and investigated earlier [4,7,11]. Recently, studies concerning the use of ceramics in MFCs have been increased. This class of materials fulfills the aforementioned properties, due to the adjustment of porosity, thickness, density, chemical stability, as well as the low cost of these materials [12]. Most of the investigations in MFCs, related to the use of ceramics, have been focusing on proton exchange membranes and reactor design [13,14]. Nevertheless, a few researchers have reported the applicability of ceramics as electrode materials [11,15,16], mainly due to the non-conductive aspect of ceramics. To address this problem, an attractive way to produce electron conducting porous ceramics is investigated based on the approach of polymer-derived ceramics (PDCs) route through polysiloxanes, where chemical and physical properties can be varied according to the molecular precursor, filler incorporation and pyrolysis conditions, generating SiOC-based ceramics [17–19]. The tailorable properties in these materials, such as specific surface area and surface characteristics, and feasibility of incorporation of conductive phases [20,21], have attracted interests for electrochemical applications as sensors [22] and as electrode materials in lithium-ion batteries and supercapacitors [20,23], but not yet explored for applications in bioelectrochemical systems (BES).

Focus on the need of new electrode materials development, new porous SiOC- ceramic anodes based on polysiloxanes were developed in the present study to offer as an effective alternative to the traditional carbon-based anodes. The applicability of the developed anodes was investigated by evaluating the performance of aqueous cathode MFCs and it is compared with MFC using commercially available carbon felt as anode material.

2. Experimental section

2.1. PDC-based anodes preparation

The PDC-based anode materials were prepared according to the procedure used for synthesizing conductive porous materials as well as hybrid materials containing metallic nanoparticles as reported previously [24,25]. In summary, the preparation starts by dissolving the polymer ceramics precursors poly(methyl silsesquioxane) (MK, Wacker Chemie AG) and poly(methyl phenyl silsesquioxane) (H44, Wacker Chemie AG) in xylene (Sigma-Aldrich Co), under constant stirring and at room temperature, followed by the dispersion of additives (MoSi$_2$, abcr GmbH and azodicarboxamide, Sigma-Aldrich Co.) and carbon-based fillers, such as graphite (KS75, IMERYL Graphite & Carbon) and carbon black (CB, Cabot). For the Ni-containing PDC-based anode material, the metal salt nickel chloride (NiCl$_2$, Alfa Aesar) was additionally used in the dispersion step along with graphite for the Ni nanoparticles formation. The cross-linking process starts with the addition of imidazole (Alfa Aesar) under constant stirring for 20 min. The materials were then casted by tape casting method and the prepared cross-linked tapes were then pyrolyzed in a pyrolysis oven (GERO Hochtemperaturöfen GmbH, Germany). The pyrolysis was performed under N$_2$ atmosphere with the heating rate of 120 K h^{-1} up to 900 °C followed by 30 K h^{-1} up to 1000 °C, with a dwelling time of 4 h. A cooling rate of 120 K h^{-1} was applied to end the pyrolysis step. The PDC-based anodes were denoted as PDC-Graphite, PDC-G-Carbon Black and PDC-G-Nickel and their compositions (wt%) are described in Table

S1 in Electronic Supplementary Information (ESI).

2.2. Materials characterization

The morphology of the resulting anode materials was observed by Scanning electron microscopy (SEM, Supra 40-Carl Zeiss, Germany). BET (Brunauer, Emmett, and Teller) specific surface areas (SSA) were determined by nitrogen adsorption isotherms measured at 77 K using the equipment Belsorp-Mini (Bel Japan, Inc.) and the materials were pretreated at 120 °C for 3 h under vacuum. The hydrophilicity/hydrophobicity characteristics were analyzed by the vapor adsorption method [26] and expressed as adsorbed vapor mass per unit area (g m^{-2}) (method description detailed in ESI). The surface wettability was assessed by water contact angle measurements, carried out on a pendant drop tensiometer (OCA25, DataPhysics, Germany). The electrical conductivity measurements were obtained by AC impedance studies in the frequency range of 1 MHz to 10 mHz with AC amplitude of 10 mV at room temperature [27] and carried out using the impedance analyzer (Impedance Measurement Unit IM6ex Zahner Electric) connected with the software THALES.

2.3. MFC configuration and operating conditions

Batch-operated aqueous cathode laboratory MFCs were used in order to enable performance comparison of as-synthesized PDC-based anode materials with the commercially available carbon felt (Panex 35, Zoltek Corporation), used as received. The anodic chamber of MFCs was made up of low cost baked clayware ceramic cylinder [28] and detailed in the ESI. The PDC-based materials developed, with a total projected surface area of 36 cm^2 and a thickness of 0.25 cm, were used as anode and placed in the inner part of the clayware cylinder. As a current collector for oxygen reduction reaction (ORR), carbon felt (Panex 35, Zoltek Corporation) was wrapped on the outer surface of the cylinder. The electrical connection between the electrodes was made with concealed copper wire, while the potential drop was measured through an external resistance of 100 Ω. A schematic representation of the MFC is shown in Fig. 1 and the four experimental setups are illustrated in Fig. S1.

A volume of 15 ml of anaerobic sludge collected from the bottom of a septic tank (volatile suspended solids of 19.9 g l^{-1} and total suspended solids of 30.2 g l^{-1}) and heat-treated (100 °C for 15 min) was added as inoculum in the anodic chamber of all the MFCs. Synthetic wastewater containing sucrose as the carbon source with a chemical oxygen demand (COD) of 2000 mg l^{-1} and pH adjusted to 7.4 was used as anolyte. The detailed composition of the synthetic sucrose based wastewater and trace metals [29,30] is provided in the ESI. All the
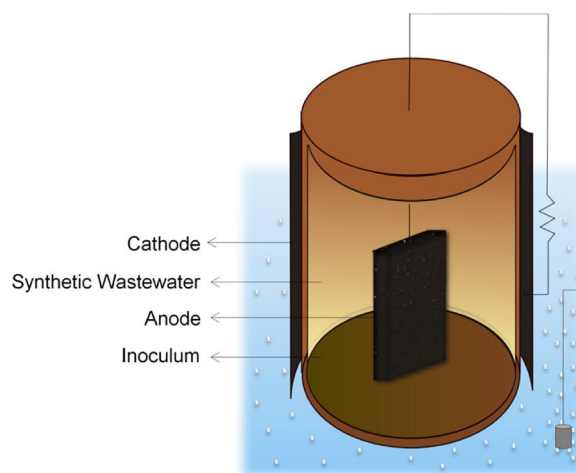

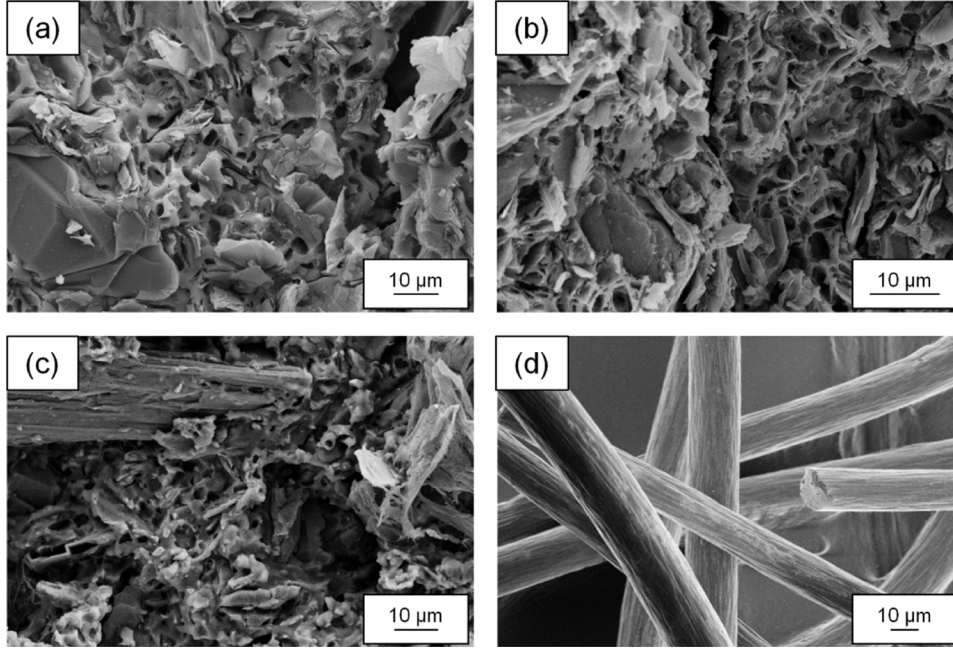**Fig. 1.** MFC setup representation and its components.

Fig. 2. SEM images of the pyrolyzed PDC-Graphite, PDC-G-Carbon Black and PDC-G-Nickel anode materials (a, b, and c respectively) at 1000 °C and commercial carbon felt (d).

MFCs were operated for 45 days under the fed-batch condition at room temperature (28–32 °C) with the fresh feeding of the anolyte after every two days.

2.4. Electrochemical measurements and analysis

The potential difference and current generated by the MFCs were monitored using a digital multimeter with data acquisition unit (Agilent Technologies, Malaysia) and power was calculated according to the Eq. (1):

$$P = I \times V \tag{1}$$

Where P is power (W), I is current (A), and V is acquired voltage (V). Anodic and cathodic potentials were measured using Ag/AgCl reference electrode (CH Instruments, Inc., RE-5B; +0.197 V *vs.* a standard hydrogen electrode, SHE). After the MFCs attained a stable potential, polarization was performed by monitoring the voltage output across various external resistances, ranging from 10 kΩ to 5 Ω, using a resistance box (GEC 05 R decade Resistance Box, Renown Systems, Kolkata, India). The voltage was recorded after every 30 min and the data was collected with the help of a data acquisition unit. Power density values were normalized to the exposed surface area of the anode materials, which gave an idea about the maximum power density it can yield. This study was also followed to obtain the relationship between the voltage and current, expressed as *IV* curves. The internal resistance of the MFC was calculated from the slope of the linear portion of the polarization plot (voltage *vs.* current). Normalized Energy Recovery (NER) was estimated according to Ge et al. and expressed in two units; based on the volume of wastewater treated and amount of organic matter removal, in terms of COD, over the time (kWh m^{-3} and kWh kg COD^{-1}, respectively) [31]. The relation is shown in Eq. (2) and Eq. (3).

$$NERv \left[\frac{kWh}{m^3} \right] = \frac{P}{wastewater\ volume} \tag{2}$$

$$NERr \left[\frac{kWh}{kg\ COD} \right] = \frac{P}{\Delta\ COD\ x\ wastewater\ volume} \tag{3}$$

Total and soluble COD were analyzed for samples collected from the anodic chamber of the MFC at a regular interval according to Standard Methods [32]. The coulombic efficiency (CE) was estimated by integrating the measured current relative to the theoretical current according to the Eq. (4) [33].

$$CE\ [\%] = \frac{M_s \int_0^t I\ dt}{Fb_{es} V_{an} \Delta COD} \tag{4}$$

Where, M_s is the molecular weight of substrate (g mol^{-1}), ΔCOD is the change in substrate concentration over a batch cycle (g L^{-1}), V_{an} is the anodic chamber liquid volume (L), F is Faraday's constant (96485 C mol^{-1}) and b_{es} is the generated electrons during each mol of substrate oxidation (mol of e- per mol of substrate^{-1}).

Any evidence of leaching of metal ions from the electrodes to the electrolyte during the operation of MFC was investigated using SOLAAR S Series atomic absorption spectrometer (Thermo Fisher Scientific, USA) according to the method described in Standard Methods [36]. Aside from this, biofilm formation on the as-synthesized anode materials was observed under an optical microscope (Light Microscope Keyence Digital, Germany) and SEM (CAM SCAM, Cambridge Scanning) at the end of the MFC operation. For this, the biofilm on the surfaces was first fixed in 2.5% glutaraldehyde for 60 min and subsequently dehydrated for 10 min in alcoholic solutions of 20, 40, 60, 80 and 100% ethanol. The materials were dried and gold coated for SEM observations.

3. Results and discussion

3.1. Physical characterization of the SiOC-based anode materials

SiOC-based anode materials were produced by tape casting technique with dimensions of 40 × 40 × 2.5 mm and pyrolyzed under nitrogen environment at 1000 °C. In order to compensate the shrinkage and weight loss of the tapes during the ceramic conversion of polymers, *ca.* 8 wt% MoSi$_2$ was used as filler based on previous studies [25]. In addition, azodicarboxiamide was used as a foaming agent to induce the formation of pores, due to its ability of introducing macro- and open porosity in the structure [34,35]. The resulting morphology of the as-prepared materials was investigated by SEM and the micrographs of the
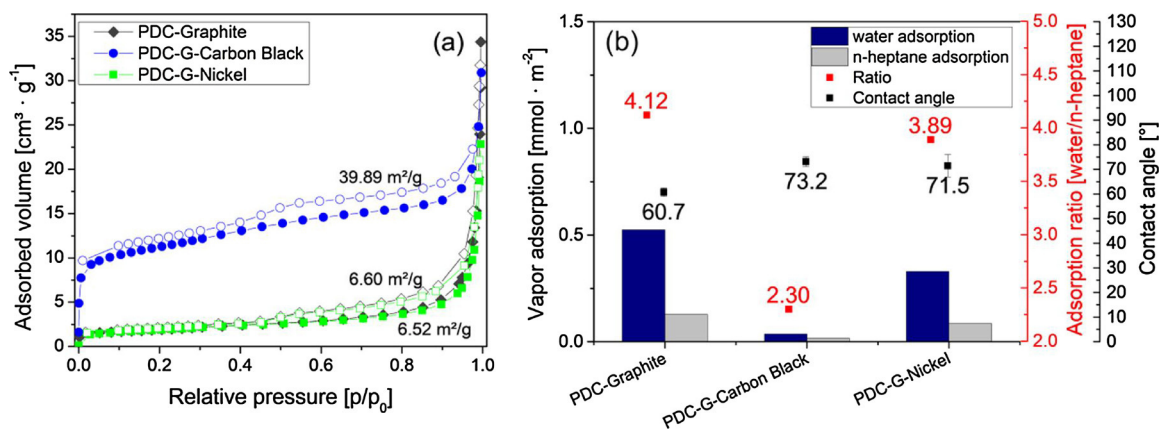
Fig. 3. Nitrogen adsorption-desorption isotherms and respective BET specific surface areas (a), water and n-heptane adsorption at 25 °C, the water/n-heptane ratio (red markers) and contact angle (black markers) of the pyrolyzed anodes prepared (b) (For interpretation of the references to color in this figure legend, the reader is referred to the web version of this article).

pyrolyzed anode materials are shown in Fig. 2. The PDC-Graphite, PDC-G-Carbon Black and PDC-G-Ni materials pyrolyzed at 1000 °C are shown in Fig. 2a–c, respectively. Fig. 2d shows the morphology of the non-treated carbon felt used as a control. From the SEM images, macropores ranging from 0.5–40 μm could be identified, which are suitable in size for accommodating bacteria, since their sizes are in the range of 200 nm to 750 μm [36]. It is also visible, because of the materials development possess, a completely distinct morphology was found compared to the carbon fibers arrangement of carbon felt. While comparing the PDC-based materials among themselves, a similar macrostructure is observed, indicating that the incorporation of carbon black or nickel particles formation is not significantly affecting the macrostructure of the PDC matrix.

The interior structures were further analyzed in terms of BET specific surface areas and surface characteristics. Fig. 3 represents the nitrogen adsorption-desorption isotherms, respective SSAs and the adsorption capacities of water and n-heptane related to SSA in combination with water contact angle measurements. In addition, the isotherm of carbon felt and contact angle values are presented in Figs. S2 and S3, respectively. As shown in Fig. 3a, PDC-G-Carbon Black, exhibited isotherms type I, that characterize micropores (pore diameter < 2 nm) filled at low relative pressures, resulting in higher specific surface areas. For PDC-Graphite and PDC-G-Nickel, isotherms type IV were observed, which is associated with mesoporous materials (pore diameter 2–50 nm) [37,38]. The PDC-based anode materials exhibited SSAs as high as $6.52–39.89 \ m^2 \ g^{-1}$, which was much higher as compared to the carbon felt ($0.032 \ m^2 \ g^{-1}$) used as a control. The higher SSAs of the PDC-based anode materials can provide more sites for reactions, enhancing electrode kinetics and hence improve the performance of MFC.

Since the hydrophobic/hydrophilic properties of a surface can affect the anodic biofilm formation, as well as the generated current intensity [39], surface characteristics and water contact angles of the synthesized anode materials were characterized (Fig. 3b). For the characterization of vapor adsorption, the materials are correlated with regard to ratios of water to n-heptane vapor adsorption, where a ratio higher than 1 indicates hydrophilicity. Materials which adsorbed more water vapor than n-heptane, indicate a higher affinity to polar vapors and hence hydrophilic surface characteristics. The additional water contact angle (WCA) measurements (Figs. 3b and S3) also confirmed the hydrophilic behavior of the PDC-based anode surfaces and hydrophobic behavior of carbon felt (WCA = 112°). The hydrophilic behavior of these PDC-based materials is related to the decomposition of methyl and phenyl moieties as a result of the pyrolysis temperature applied (1000 °C) [19]. The materials differ in the degree of hydrophilicity, evaluated by the vapor uptake ratio (water/n-heptane), and PDC-G-Carbon Black

showed the lower hydrophilicity, which is mainly due to the higher carbon content on its composition.

The hydrophilicity was found to be beneficial to bacterial adherence [39], which demonstrates an advantage of PDC materials when compared to hydrophobic carbon materials. This positive effect on the performance of MFC is also supported by Chang et al. and Zhao et al., while using carbon-based surface-modified electrodes [40,41]. The relevance of hydrophilic surfaces is attributed to favorable biosorption of bacteria on the surface of electrodes providing a more suitable environment for bacterial growth [40,41].

In order to evaluate the stability of the anodes, a preliminary study of dry weight variation in a phosphate buffer solution (PBS, pH 7), at room temperature over a period of 4 weeks was performed. For this test, a material with a higher amount of $NiCl_2$ in the composition (5 wt %) was considered. The materials revealed appropriate stability, with weight loss/increase lower than 3% (Fig. S4). The increased weight for the PDC-G-Ni material can be accounted to the formation of a passive layer (oxide) on the exposed surface.

3.2. Electrical performance of MFC

Applicability and performance of the novel anode materials based on PDC were evaluated in terms of power production. The presence of active exo-electrogenic bacteria in mixed anaerobic consortia was endorsed by the fact that all the four MFCs started showing voltage from the very first day after its start-up. Thus, reduced time for anodic acclimatization was observed for all the MFCs. After the initial start-up duration of 13–15 days, stable performance in terms of electrical output and organic matter removal was observed for the next 15 cycles for better replication of datasets. The measured electrical conductivity by EIS and anode's parameters during the stable operation of the MFC are summarized in Table 1. The average operating voltage of 219 ± 15 mV was achieved under the steady-state operating condition and over an external resistance of 100 Ω for MFC with PDC-G-Carbon Black as anode. This value was comparably higher than the values obtained by the MFC with PDC-Graphite (150 ± 15 mV), the MFC with PDC-G-Nickel (18 ± 7 mV) and the control MFC with carbon felt (213 ± 7 mV). In addition, the pH of the anolyte was adjusted to about 7.4, whereas in the catholyte the pH ranged between 7.5 and 8.0 for the entire course of the study.

Fig. 4a-b represents the power generation results according to IV curves and polarization curves. Power generation normalized to the volume of the MFC is additionally displayed in Fig. S5. The polarization data showed that low activation loss was observed and the total internal resistance of MFC with PDC-G-Carbon Black was found to be 165 Ω, comparably lower than MFC with the PDC-Graphite anode (217 Ω),

Table 1
Electrical conductivity measured by impedance and anode parameters during the operation of the MFCs.

Anode material	PDC- Graphite	PDC-G-Carbon Black	PDC-G-Nickel	Carbon Felt
Electrical conductivity [$S \cdot cm^{-1}$]	0.099	0.176	0.102	0.761
Maximum OV [mV]	162	231	21	220
Maximum OCV[mV]	789	824	239	811
Anode potential [mV]	−421	−439	−12	−447
Maximum power density [$mW \cdot m^{-2}$]	144	211	30	111
Maximum current density [$mA \cdot m^{-2}$]	447	542	288	277
Internal resistance [Ω]	217	165	286	373

MFC with PDC-G-Nickel (286 Ω) and the control MFC with carbon felt (373 Ω). Besides, the MFC operated with PDC-G-Carbon Black as anode could generate a maximum power density of 211 mW m^{-2}, which was 46.5%, 603.3% and 90.1% higher compared to that of MFC with PDC-Graphite anode (144 mW m^{-2}), MFC with PDC-G-Nickel (30 mW m^{-2}) and the control MFC with carbon felt (111 mW m^{-2}), respectively (Fig. 4, Table 1).

Based on the results obtained, it may be concluded that the MFC with the anode PDC-G-Carbon Black had higher electron transfer efficiency with reduced ohmic resistance, due to which it could generate higher power production as compared to the other three MFCs by recovering additional coulombs. A two-fold increase in the maximum current density and maximum power density was achieved by the anode PDC-G-Carbon Black compared to commercial carbon felt reveals a significant improvement in the performance of MFC. This improved performance can be related to the porous structure, hydrophilic surface and highest SSA characterized in this PDC-based anode material. The lower power production of the MFC with PDC-G-Nickel can be attributed to the leaching of nickel over time during operation of MFC. The AAS results further confirmed the supposition by giving a positive test result (0.9 ± 0.1 µg/L) for the presence of nickel in the anolyte of MFC, over any course of time. During the continuous operation of the MFC, fatty acids are produced while organic matter degradation and fermentation processes, which results in electrolyte acidification. The acidic conditions could gradually lead to the dissolution of nickel from the electrode. The solution with leached Ni(II) from the PDC-G-Nickel acts as electron acceptor in the anode chamber and reduces down to pure Ni(0) with a redox potential of -0.25 V (Eq. (5)), because of this the power production was compromised for this MFC.

$$Ni^{2+} \, (aq) + 2e^- \rightarrow Ni^\circ \, (s) \qquad (5)$$

On the other hand, the carbon nanotubes formation at this particular Ni-containing material (Fig. S6) could have been, in a certain level, toxic to the exoelectrogenic bacteria used in this study and inhibit the growth of biomass [43], which further decreases the performance of MFC.

Although the control MFC with graphite felt showed higher electrical conductivity value than the PDC-based anodes, the improved performance achieved suggests that the contribution of porosity and surface properties of the materials plays a crucial role in the biofilm development, influencing the overall power production. The performance obtained by the PDC-G-Carbon Black is in the range of previous studies conducted using 3D-electrode materials for Bioelectrochemical Systems (Table S2).

3.3. Wastewater treatment in MFC

In order to analyze the performance of electricity generation focusing on energy, maximum NER was estimated (Fig. 5a). The maximum NER_v in the MFC with PDC-G-Carbon Black was found to be substantially enhanced, with a value of 0.43 kW h m^{-3}, which was around 95.4% higher than the MFC with carbon felt as control (0.22 kW h m^{-3}), and 48.3%, 616.7% higher than the MFC with PDC-Graphite (0.29 kW h m^{-3}) and PDC-G-Nickel (0.06 kW h m^{-3}), respectively. For the maximum NER_r, a similar trend was observed, however, it differs in the percentage of enhancement. The MFC with PDC-G-Carbon Black anode showed the highest NER_r of 0.26 kW h kg COD^{-1}, which was 100% higher than the MFC using carbon felt as control anode (0.13 kW h kg COD^{-1}). Additionally, an increase of 52.9% and 420.0% was found for the MFCs with PDC-Graphite (0.17 kW h kg COD^{-1}) and PDC-G-Nickel (0.05 kW h kg COD^{-1}), when compared to PDC-G-Carbon Black (0.26 kW h kg COD^{-1}).

Bi-functional property of MFC as an efficient system for the treatment of wastewater and simultaneous bio-energy production has been documented extensively [42]. Wastewater treatment efficiency, mostly comprises of removal efficiency of COD, was monitored for 15 fed-batch cycles with each cycle having a reaction time of 2 days. The COD removal efficiencies of 86.3 ± 0.7%, 83.3 ± 1.9%, 60.0 ± 2.5% and 85.4 ± 0.7% were found in MFC with PDC-Graphite, MFC with PDC-G-Carbon Black, MFC with PDC-G-Nickel and the control MFC with carbon felt, respectively (Fig. 5b). Except for the Ni-containing material, all the COD removal rates were comparable with the values reported for clayware based MFCs in the literature [43,44].
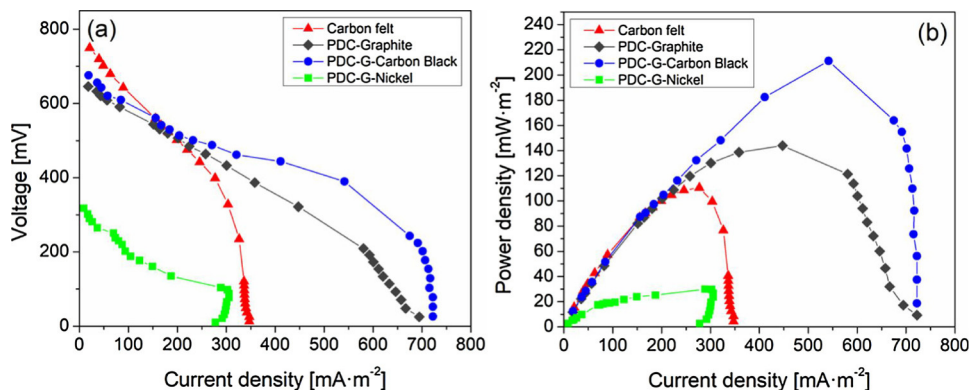

Fig. 4. Polarization curves (a) and power density *versus* current density curves (b) of the MFCs with PDC-based anodes and carbon felt normalized to the projected anode area.
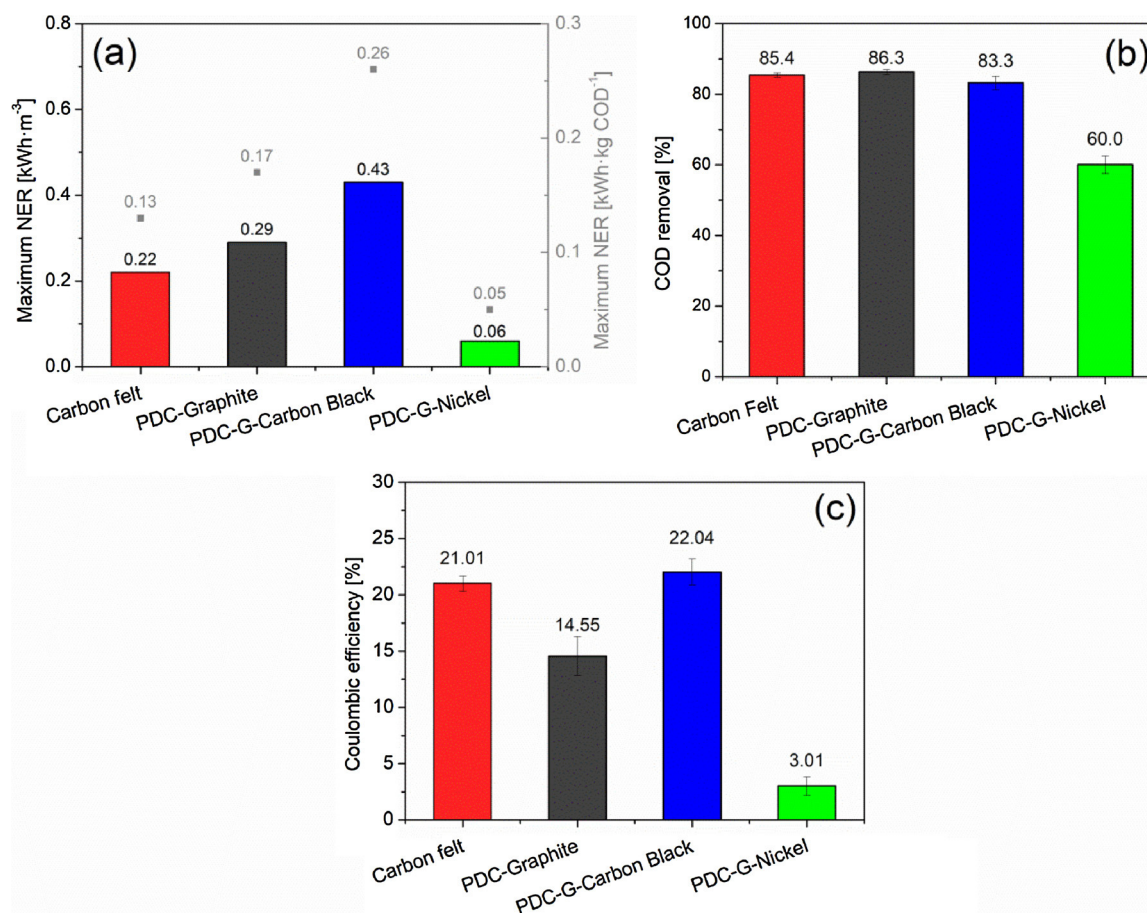
Fig. 5. Maximum NER (a), COD removal rate (b), coulombic efficiency (c) of the MFCs with PDC-based anodes and carbon felt.

The CE was estimated to further evaluate the accountability of PDC-based anode materials for MFC applications. The CE values are a passive index of correlation between the total current output from the MFCs and the COD removal values, which reflect the overall performance of the MFCs. The MFC with PDC-G-Carbon Black showed a CE of $22.04 \pm 1.16\%$, which was higher than that obtained from the MFC with PDC-graphite ($14.55 \pm 1.73\%$) and control MFC with graphite felt ($21.01 \pm 0.70\%$) and almost 7 times higher than the MFC with PDC-G-Nickel ($3.01 \pm 0.81\%$; Fig. 5c). Thus, the applicability of PDC-G-Carbon Black as a better alternative anode material for MFC is established with promising sustainable wastewater treatment capability along with the benefit of tapping the maximum available energy reserve from wastewater.

3.4. Biofilm on anode surfaces

The increase in current and power generation can be associated with an electrochemically active biofilm formed on solid electrodes. To confirm and evaluate the biofilm formation on the anode materials, the materials were observed under a digital microscope and SEM after 45 days of operation. Fig. 6 demonstrates the biofilm growth on the surfaces, confirming the biocompatibility of PDC-based materials to allow bacterial attachment.

A distinctive biofilm formation was observed in the images of each material. Especially for the Ni-containing one, that shows a poor biofilm formation and presented a lower power performance compared to the other PDC-based materials and carbon felt. From the SEM images (Fig. S7), it was further confirmed that the meso-macroporous structure of the PDC-anode materials provided an available surface for bacterial growth, superior to the carbon felt structure. Dense colonization was also observed and distributed on cracks. Furthermore, short, rod-shaped bacteria attached could also be visualized.

4. Conclusions

The SiOC-based anodes prepared in this work, by the polymer-derived ceramics route, were applied in MFC for the first time. The porous materials presented micro-meso and macropores and hydrophilic surfaces. The electrodes allowed bacterial attachment and showed a performance compared to a commercially available carbon felt, resulting in a two-fold increase in the maximum current density and power density. In terms of wastewater treatment efficiency, a chemical oxygen demand removal of about 85% was achieved. The highest performance, obtained by the PDC-G-Carbon Black, was also compared to previous studies in bio-electrochemical systems, confirming its applicability as novel anode material. Lastly, this study provides the first findings of SiOC-based anode ceramic materials to be considered as in future material development as promising electrodes for MFC technology.

Conflict of interests

There are no conflicts to declare.

Data availability

The datasets generated during and/or analyzed during the current work are available from the corresponding author on reasonable request.
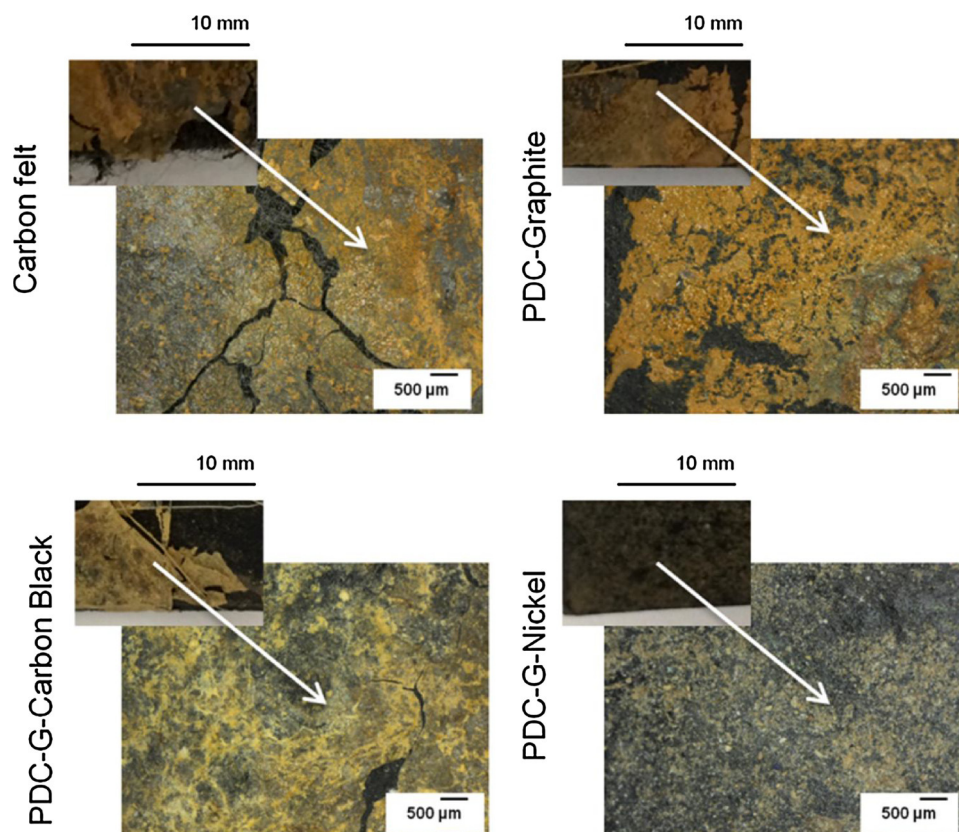
Fig. 6. Digital images of biofilm on carbon felt and PDC-based anodes after 45 days of MFC performance.

Acknowledgments

Appendix A. Supplementary data

Supplementary material related to this article can be found, in the online version, at doi:https://doi.org/10.1016/j.bej.2019.04.004.

References

[1] B.E. Logan, K. Rabaey, Conversion of wastes into bioelectricity and chemicals by using microbial electrochemical technologies, Science 337 (2012) 686–690.

[2] A. Janicek, Y. Fan, H. Liu, Design of microbial fuel cells for practical application: a review and analysis of scale-up studies, Biofuels 5 (2014) 79–92.

[3] V.B. Oliveira, M. Simoes, L.F. Melo, A.M.F.R. Pinto, Overview on the developments of microbial fuel cells, Biochem. Eng. J. 73 (2013) 53–64.

[4] A. ElMekawy, H.M. Hegab, X. Dominguez-Benetton, D. Pant, Internal resistance of microfluidic microbial fuel cell: challenges and potential opportunities, Bioresour. Technol. 142 (2013) 672–682.

[5] A. Mehdinia, E. Ziaei, A. Jabbari, Multi-walled carbon nanotube/SnO2 nano-composite: a novel anode material for microbial fuel cells, Electrochim. Acta 130 (2014) 512–518.

[6] C. Santoro, C. Arbizzani, B. Erable, I. Ieropoulos, Microbial fuel cells: from fundamentals to applications. a review, J. Power Sources 356 (2017) 225–244.

[7] M.H. Zhou, M.L. Chi, J.M. Luo, H.H. He, T. Jin, An overview of electrode materials in microbial fuel cells, J. Power Sources 196 (2011) 4427–4435.

[8] H.T. Chou, H.J. Lee, C.Y. Lee, N.H. Tai, H.Y. Chang, Highly durable anodes of microbial fuel cells using a reduced graphene oxide/carbon nanotube-coated scaffold, Bioresour. Technol. 169 (2014) 532–536.

[9] Y. Hindatu, M.S.M. Annuar, A.M. Gumel, Mini-review: anode modification for improved performance of microbial fuel cell, Renew. Sustain. Energy Rev. 73 (2017) 236–248.

[10] H.R. Yuan, L.F. Deng, Y. Chen, Y. Yuan, MnO2/Polypyrrole/MnO2 multi-walled-nanotube-modified anode for high-performance microbial fuel cells, Electrochim. Acta 196 (2016) 280–285.

[11] R. Thorne, H.N. Hu, K. Schneider, P. Bombelli, A. Fisher, L.M. Peter, A. Dent, P.J. Cameron, Porous ceramic anode materials for photo-microbial fuel cells, J. Mater. Chem. 21 (2011) 18055–18060.

[12] J. Winfield, I. Gajda, J. Greenman, I. Ieropoulos, A review into the use of ceramics in microbial fuel cells, Bioresour. Technol. 215 (2016) 296–303.

[13] I.M. Jimenez, J. Greenman, I. Ieropoulos, Electricity and catholyte production from ceramic MFCs treating urine, Int. J. Hydrogen Energ. 42 (2017) 1791–1799.

[14] V. Yousefi, D. Mohebbi-Kalhori, A. Samimi, Ceramic-based microbial fuel cells (MFCs): a review, Int. J. Hydrogen Energ. 42 (2017) 1672–1690.

[15] D. Hidalgo, T. Tommasi, V. Cauda, S. Porro, A. Chiodoni, K. Bejtka, B. Ruggeri, Streamlining of commercial Berl saddles: a new material to improve the performance of microbial fuel cells, Energy 71 (2014) 615–623.

[16] D. Massazza, R. Parra, J.P. Busalmen, H.E. Romeo, New ceramic electrodes allow reaching the target current density in bioelectrochemical systems, Energy Environ. Sci. 8 (2015) 2707–2712.

[17] P. Colombo, G. Mera, R. Riedel, G.D. Soraru, Polymer-derived ceramics: 40 years of research and innovation in advanced ceramics, J. Am. Ceram. Soc. 93 (2010) 1805–1837.

[18] E. Ionescu, H.J. Kleebe, R. Riedel, Silicon-containing polymer-derived ceramic nanocomposites (PDC-NCs): preparative approaches and properties, Chem. Soc. Rev. 41 (2012) 5032–5052.

[19] T. Prenzel, M. Wilhelm, K. Rezwan, Pyrolyzed polysiloxane membranes with tailorable hydrophobicity, porosity and high specific surface area, Microporous Mesoporous Mater. 169 (2013) 160–167.

[20] M.S. Kolathodi, L. David, M.A. Abass, G. Singh, Polysiloxane-functionalized graphene oxide paper: pyrolysis and performance as a Li-ion battery and super-capacitor electrode, RSC Adv. 6 (2016) 74323–74331.

[21] P. Moni, M. Wilhelm, K. Rezwana, The influence of carbon nanotubes and graphene oxide sheets on the morphology, porosity, surface characteristics and thermal and electrical properties of polysiloxane derived ceramics, RSC Adv. 7 (2017) 37559–37567.

[22] A. Karakuscu, A. Ponzoni, P.R. Aravind, G. Sberveglieri, G.D. Soraru, Gas sensing behavior of mesoporous SiOC glasses, J. Am. Ceram. Soc. 96 (2013) 2366–2369.

[23] V.S. Pradeep, D.G. Ayana, M. Graczyk-Zajac, G.D. Soraru, R. Riedel, High rate capability of SiOC ceramic aerogels with tailored porosity as anode materials for Li-ion batteries, Electrochim. Acta 157 (2015) 41–45.

[24] F. Schlüter, J. Meyer, M. Wilhelm, K. Rezwan, Hierarchical emulsion based hybrid ceramics synthesized with different siloxane precursor and with embedded nickel nanoparticles, Colloids Surf. A Physicochem. Eng. Asp. 492 (2016) 160–169.

[25] J.F. Drillet, M. Adam, S. Barg, A. Herter, D. Koch, V.M. Schmidt, M. Wilhelm, Development of a novel Zinc/Air fuel cell with a Zn foam anode, a PVA/KOH membrane and a MnO_2/SiOC-based air cathode, ECS Trans. 28 (2010) 13–24.

[26] T. Prenzel, T.L.M. Guedes, F. Schluter, M. Wilhelm, K. Rezwan, Tailoring surfaces of hybrid ceramics for gas adsorption - from alkanes to CO_2, Sep. Purif. Technol. 129 (2014) 80–89.

[27] M. Prabu, S. Selvasekarapandian, A.R. Kulkarni, S. Karthikeyan, G. Hirankumar, C. Sanjeeviraja, Ionic transport properties of $LiCoPO_4$ cathode material, Solid State Sci. 13 (2011) 1714–1718.

[28] K.K. Türk, I. Kruusenberg, E. Kibena-Põldsepp, G.D. Bhowmick, M. Kook, K. Tammeveski, L. Matisen, M. Merisalu, V. Sammelselg, M.M. Ghangrekar, A. Mitra, R. Banerjee, Novel multi walled carbon nanotube based nitrogen impregnated Co and Fe cathode catalysts for improved microbial fuel cell performance, Int. J. Hydrogen Energ. 43 (2018) 23027–23035.

[29] M.M. Ghangrekar, S.R. Asolekar, S.G. Joshi, Characteristics of sludge developed under different loading conditions during UASB reactor start-up and granulation, Water Res. 39 (2005) 1123–1133.

[30] G.S. Jadhav, M.M. Ghangrekar, Performance of microbial fuel cell subjected to variation in pH, temperature, external load and substrate concentration, Bioresour. Technol. 100 (2009) 717–723.

[31] Z. Ge, J. Li, L. Xiao, Y.R. Tong, Z. He, Recovery of electrical energy in microbial fuel cells, Environ. Sci. Technol. Lett. 1 (2014) 137–141.

[32] APHA, Standard Methods for the Examination of Water and Wastewater, 20th edition, APHA American Public Health Association, Washington, DC, USA, 1998.

[33] B.E. Logan, B. Hamelers, R.A. Rozendal, U. Schrörder, J. Keller, S. Freguia, P. Aelterman, W. Verstraete, K. Rabaey, Microbial fuel cells: methodology and technology, Environ. Sci. Technol. 40 (2006) 5181–5192.

[34] M. Fukushima, P. Colombo, Silicon carbide-based foams from direct blowing of polycarbosilane, J. Eur. Ceram. Soc. 32 (2012) 503–510.

[35] A. Idesaki, P. Colombo, Synthesis of a Ni-Containing porous SiOC material from polyphenylmethylsiloxane by a direct foaming technique, Adv. Eng. Mater. 14 (2012) 1116–1122.

[36] S.W. Lee, B.Y. Jeon, D.H. Park, Effect of bacterial cell size on electricity generation in a single-compartment microbial fuel cell, Biotechnol. Lett. 32 (2010) 483–487.

[37] S. Brunauer, L.S. Deming, W.E. Deming, E. Teller, On a theory of the van der Waals adsorption of gases, J. Am. Chem. Soc. 62 (1940) 1723–1732.

[38] IUPAC, Manual of Symbols and Terminology for Physicochemical Quantities and Units, London Butterworths, Bristol, UK, 1972.

[39] K. Guo, S. Freguia, P.G. Dennis, X. Chen, B.C. Donose, J. Keller, J.J. Gooding, K. Rabaey, Effects of surface charge and hydrophobicity on anodic biofilm formation, community composition, and current generation in bioelectrochemical systems, Environ. Sci. Technol. 47 (2013) 7563–7570.

[40] S.H. Chang, J.S. Liou, J.L. Liu, Y.F. Chiu, C.H. Xu, B.Y. Chen, J.Z. Chen, Feasibility study of surface-modified carbon cloth electrodes using atmospheric pressure plasma jets for microbial fuel cells, J. Power Sources 336 (2016) 99–106.

[41] Y. Zhao, Y. Ma, T. Li, Z.S. Dong, Y.X. Wang, Modification of carbon felt anodes using double-oxidant HNO_3/H_2O_2 for application in microbial fuel cells, RSC Adv. 8 (2018) 2059–2064.

[42] Z. Du, H. Li, T. Gu, A state of the art review on microbial fuel cells: a promising technology for wastewater treatment and bioenergy, Biotechnol. Adv. 25 (2007) 464–482.

[43] A.N. Ghadge, D.A. Jadhav, H. Pradhan, M.M. Ghangrekar, Enhancing waste activated sludge digestion and power production using hypochlorite as catholyte in clayware microbial fuel cell, Bioresour. Technol. 182 (2015) 225–231.

[44] D.A. Jadhav, A.N. Ghadge, M.M. Ghangrekar, Simultaneous organic matter removal and disinfection of wastewater with enhanced power generation in microbial fuel cell, Bioresour. Technol. 163 (2014) 328–334.